AEROELASTIC STABILITY OF THE MCDONNELL DOUGLAS ADVANCED BEARINGLESS ROTOR

Khanh Nguyen
Aerospace Engineer
NASA Ames Research Center
Moffett Field, CA

Michael McNulty, Vaidyanathan Anand, and Dan Lauzon
Members of Technical Staff
McDonnell Douglas Helicopter Company
Mesa, AZ

Abstract

An aeroelastic stability investigation was conducted on the full-scale McDonnell Douglas advanced bearingless rotor in the NASA Ames 40- by 80-Foot Wind Tunnel. Test results indicated stable rotor operation at all flight conditions tested. The blade inplane damping depends strongly on the collective pitch, with the damping level increasing significantly with collective pitch increase. Issues encountered during the stability data acquisition and reduction are discussed. Both the UMARC and DART results compare well with the measured inplane damping for this rotor.

Introduction

The introduction of bearingless rotor designs have posed new challenges to the analysis of rotor aeroelasticity. Bearingless rotors are characterized by flexural members that allow for blade flap, lead-lag, and pitch motions without discrete hinges or bearings. The elimination of hinges and bearings significantly reduces the complexity of rotor hub designs leading to improved maintainability and manufacturability requirements. Advances in composite materials, manufacturing techniques, and rotorcraft analytical techniques have made bearingless rotor designs feasible. The physical simplicity of these designs, however, complicates the analysis of rotor aeroelasticity due to the redundant load paths, complex bending-torsion and geometrical couplings, and material nonlinear characteristics. These rotors are susceptible to air and ground resonances making aeroelastic stability predictions vital in the development of bearingless rotors. Reliable predictions often depend on the validation of the analysis with a comprehensive database, which for modern bearingless rotors, is virtually absent in the published literature.

Presented at the American Helicopter Society 49th Annual Forum, St. Louis, Missouri, May 19-21, 1993. *Copyright © 1993 by the American Helicopter Society, Inc. All rights reserved.*

Over the past two decades, several rotor development projects focused on bearingless rotors without additional dampers (Refs. 1-3). In addition to the inherent structural damping, the blade inplane damping was achieved through aeroelastic tailoring, such as pitch-lag coupling. However, test results revealed that the complex aeroelastic behavior of such rotors undermined the anticipated benefits of aeroelastic tailoring and rendered the rotor systems inadequate for ensuring aeromechanical stability over a complete range of rotor speed and vehicle operating conditions. Until now, the only damperless bearingless main rotor that was flight tested was the Boeing Vertol designed Bearingless Main Rotor (Ref. 2) which possessed marginal aeromechanical stability characteristics.

Virtually all bearingless rotors being built and tested today employ lead-lag dampers, typically made of elastomeric materials. The major components of a modern bearingless rotor are the blades, the flexbeams, the wrap-around pitchcases (or torque tubes), and the snubber-damper assemblies. The bearingless rotors described in Refs. 4-6 typify this design. The snubber-damper assembly is a unique feature of modern bearingless rotors. The shear lag dampers, the snubber design, and the pitchcase and flexbeam designs dominate the aeroelastic and aeromechanical stability of modern bearingless rotors. References 7-9 document other investigations of bearingless rotor stability.

The first modern bearingless rotor designs to fly were the Model 680 from Bell Helicopter Textron (BHT) and the HARP from McDonnell Douglas. Other bearingless rotors have flown since then, including the BHT ALR and the 4BW, the MBB BO-108, and the Kawasaki bearingless rotor (Ref. 10). The McDonnell Douglas MD Explorer and the Boeing-Sikorsky Comanche represent the latest bearingless rotor designs.

In a cooperative research program, NASA Ames Research Center and McDonnell Douglas Helicopter Company conducted a joint wind tunnel investigation of the McDonnell Douglas Advanced Rotor Technology (MDART) rotor to provide a much needed database for modern bearingless rotor research. Figure 1 shows the rotor

installed in the NASA Ames 40- by 80- Foot Wind Tunnel test section. The joint NASA-McDonnell Douglas wind tunnel test program aimed to measure the rotor aerodynamic performance, handling qualities, blade and hub loads, control power requirements, aeroelastic stability, acoustic characteristics, and responses to higher harmonic control inputs. The MDART rotor was tested from hover to airspeeds in excess of 200 kts and up to 10,000 lb of thrust, corresponding to a thrust coefficient to solidity ratio (C_T/σ) of 0.13. Reference 11 describes the overall wind tunnel test program.

A primary objective of this investigation was to determine the aeroelastic stability of the MDART rotor for an extensive set of simulated flight conditions. The test data form the first full-scale aeroelastic stability database for a modern bearingless rotor in both hover and forward flight. This paper presents the aeroelastic stability results from this test program and the results of a correlation study comparing the test data with two rotorcraft analyses: the University of Maryland Advanced Rotorcraft Code or UMARC and the McDonnell Douglas Dynamic Analysis Research Tool or DART analysis.

Test Hardware

The MDART rotor is a pre-production MD Explorer rotor. The 34-foot diameter rotor is a modern five-bladed, soft-inplane bearingless design for a 5800 lb helicopter. The design cruise speed is 150 kts at a nominal C_T/σ of 0.075. The modern HH-10 airfoil section extends from the blade attachment to the 80 percent blade radial station, and the outboard section uses the HH-06 airfoil section. The blade tip planform is parabolic.

The flexbeam is a flexural member that connects the blade to the hub and covers 20 percent of the blade radius. The flexbeam carries the large centrifugal load and allows for the blade flap, lead-lag, and pitch motions. The pitchcase, a relatively rigid tube wrapped around the flexbeam, connects the blade to the control system through the pitch link and transfers the pitch inputs to the blade. The snubber acts as a pivot for the flap motions at the pitchcase inboard end and allows the pitchcase to rotate in pitch. The snubber also reacts the majority of the pitch-link load and provides a load path for the pitchcase vertical and shear forces to the hub. A pair of shear lag dampers, made of elastomeric materials, is mounted between the snubber and the pitchcase to provide auxiliary damping to the blade inplane motion.

In the test program, the rotor was installed on the McDonnell Douglas Large Scale Dynamic Rig (LSDR) in the Ames 40- by 80-Foot Wind Tunnel (see Fig. 1). The LSDR lower housing contained a 1500 hp electric motor and transmission system. The upper housing contained the rotor balance and the hydraulic servo-actuators for the control system. These actuators have a high rate, limited stroke capability that was used for dynamic excitation to the nonrotating swashplate. This high speed control system is capable of excitation frequencies above 40 Hz and was used in the test program for higher harmonic control inputs and for stability testing.

Stability Data Acquisition and Reduction

Standard techniques were used to acquire the stability data, with precautions taken to minimize the effects of varying damper strain levels. Once the desired steady state operating condition was achieved, the swashplate was excited at the fixed system regressive lag mode frequency. This resulted in blade pitch oscillations at the fundamental chordwise frequency in the rotating frame. The resulting oscillating airloads caused the blade to flap, and the blade inplane motions were excited through the Coriolis coupling with the flapping motions. The amplitude of the swashplate oscillation was increased to a predetermined value or until a load limit was reached at any of the instrumented blade stations.

The termination of the excitation signal occurred shortly after the beginning of the digital data acquisition with the Signal Analysis System (SAS). The SAS recorded 16 channels simultaneously for eight seconds at a sampling rate of 128 samples per second. The recorded signals included the flexbeam chordwise bending signal at 0.096R (where R is the blade radius) and the damper chordwise displacement. The transient response of the chordwise bending moment was analyzed on-line using a moving block method to provide a stability data trend. As a check on the repeatability of the data, stability measurements were repeated at all test conditions. If high loads were a concern at a particular test condition, the first stability point was often acquired at a lower level of excitation than usual; then the level would be increased for subsequent stability data acquisition points.

The SAS recorded signals were later transferred to a MicroVax for post-test analysis. The transient decay time histories from the flexbeam chordwise bending gauge at 0.096R and the damper displacement were analyzed using both a moving block method (Ref. 12) and a time domain transient analysis, providing four damping estimations per stability data point. The moving block method employs a Fast Fourier Transform algorithm with a Hanning window. The block sizes are optimized to minimize leakage while being small enough to provide an accurate curve-fit to the natural logarithm of the moving block function, defined as the magnitude of the finite Fourier transform of the transient signal computed at the rotating blade fundamental chordwise frequency.

The other method is a time domain transient analysis developed by Wilcox and Crawford (Ref. 13) for modal parameter estimation from free-oscillation data acquired in

fixed-wing flutter testing. This method was adapted to analyze multi-mode transient decay records for rotor aeroelastic stability testing. The transient analysis in general performs better than the moving block method for transient decay records with high damping levels and with modes with small frequency separation. For transient records with low damping levels, either method yields a consistent set of results. The damper motions consistently indicate somewhat higher damping levels and have more scatter than do the chordwise bending signals. The difference in the damping estimates between two measurements on the same structure is due to the nonlinear characteristics of the damper. McDonnell Douglas has encountered this phenomenon in previous bearingless rotor tests.

The aeroelastic stability database for the test program consists of 283 data points covering approximately 150 different flight conditions. Stability data were acquired for both hover and forward flight conditions, including RPM sweeps, and thrust and shaft angle sweeps at different airspeeds. Special precautions taken in the data acquisition and data reduction techniques provided confidence in the stability test results.

Analytical Models

Stability results from two analyses will be presented and correlated with the test data. The first analysis is UMARC from the University of Maryland (Ref. 14) and the second is the McDonnell Douglas DART. DART is the standard rotor dynamics analysis code at MDHC and was used extensively in the design and development of the MDART rotor, as well as the Apache and the MD 500 rotor systems. DART is the product of over two decades of development and is capable of analyzing a wide range of structural dynamic problems, while remaining compact in terms of code size. UMARC is a modern finite element code, capable of analyzing bearingless rotors with redundant load paths, and includes advanced unsteady aerodynamics and vortex wake modeling.

UMARC Analysis

The blade structural model in UMARC is an elastic beam, undergoing flap bending, lead-lag bending, elastic twist, and axial deflection. The finite element method based on Hamilton's principle is employed to discretize the blade into a finite number of beam elements. Each beam element has fifteen degrees-of-freedom and consists of two end nodes and three internal nodes. The six degrees-of-freedom at each end node are: displacements and slopes for the flap and lead-lag bending, and displacements for the elastic twist and axial deflection. There are two internal nodes for the axial degree-of-freedom, and one internal node for the elastic twist motion. The formulation of the governing equations is developed for nonuniform blades having pre-twist, pre-pitch, precone, and chordwise offsets from the blade pitch axis for the loci of the center-of-mass and aerodynamic center, and the tensile and elastic axes.

The blade boundary conditions and the connectivity between beam elements were incorporated into UMARC to model the MDART rotor. The blade and flexbeam formed one load path connected to the hub, and the pitchcase formed another load path connecting the blade to the control system and the snubber-damper assembly. The flexbeam is cantilevered to the hub. The pitchcase inboard end is free, restrained by the snubber-damper assembly and the pitch-link, modeled as discrete springs and linear viscous dampers. At the blade-flexbeam-pitchcase connection, continuity of displacements and slopes for flap and lead-lag bending and displacements for elastic twist and axial deflections was imposed.

The airloads were calculated using the quasi-steady aerodynamic model. For steady inflow calculations, Landgrebe's prescribed wake model, adapted from CAMRAD (Ref. 15), was used. The coupled blade responses and the trim control settings were solved for a simulated wind tunnel condition. The rotor shaft orientation was set to the test condition value, and the rotor was trimmed to a prescribed thrust and zero mean pitching and rolling hub moments.

The aeroelastic stability calculation is based on the linearization of the blade equations about the trim values. Modal reduction, using the blade coupled natural vibration modes, is applied to the linearized blade equations. The resulting modal equations contain periodic coefficients, requiring the application of the Floquet-Lyapunov Theory for stability analysis. Using this method, the stability of the rotor system is determined by the characteristic exponents of the state transition matrix (Ref. 16). Another popular method for stability analysis is the Constant Coefficient Approximation method, in which the state transition matrix is approximated as the matrix exponential of the time-averaged Jacobian of the blade equations. In effect, this method reduces the analysis of periodic systems to those with constant coefficients and hence obviates the computation of the state transition matrix. The stability of the system is determined directly from the eigenvalues of the time-averaged values of the Jacobian. Both methods were used to investigate the forward flight stability of the MDART rotor.

DART Analysis

DART is a program that analyzes the dynamics of multiple degrees of freedom connected through masses, dampers, springs and linear constraints. Such a system can be analyzed for linear stability, frequency and transient responses. The DART transient analysis is capable of including nonlinear effects, such as stall.

Specialized structural and aerodynamic modules are available to accept rotor blade input specifications in a standard format and then convert them into appropriate models accessible by the core program. The results represent the discretized dynamics due to the coupled flap-lag-torsion deformation of a rotor blade.

The structural pre-processor automatically generates a standard model for the primary load along the blade for five coupled motions at each blade radial station: displacements and slopes for flap and lead-lag, and torsion displacement. The analysis completes the model by filling in the connections between the blade root and the hub as appropriate to the rotor. For the MDART rotor, the standard model is continued inboard along the flexbeam to the hub. The additional load paths are then modeled by adding elements that connect the blade root to the pitchcase, the snubber-damper assembly and the hub on one side, and the pitchcase to the pitch link and control input on the other side. The structural pre-processor also allows input of a steady deflected blade shape for linearization.

Both linear and nonlinear aerodynamic options are available. Linear aerodynamics is used for stability and frequency response analysis, while the nonlinear aerodynamic options, which include an airfoil table look-up and dynamic stall modeling, are available for time-history response analysis.

Stability analysis is performed in the rotating frame. In forward flight, the perturbation matrices are formed in the rotating frame at an airspeed corresponding to a specific blade azimuthal position. This method is different from the Constant Coefficient Approximation method. To include periodically time-varying coefficients and nonlinear effects, the transient analysis remains an option. The transient responses are processed using a moving block method to estimate the system damping values.

Table 1 presents the natural frequency calculations for the six lowest blade modes for the MDART rotor using UMARC and DART analyses. These modes were used in UMARC for both trim and stability calculations and in DART for stability computations.

Results and Discussion

The behavior of the blade fundamental chordwise mode dominates the aeroelastic stability of the rotor system. The coupling of this mode with the in-plane hub motions can cause dynamic instabilities known as ground and air resonance. Successful prevention of these instabilities depends on the damping levels of the first chordwise mode and of the rotor support system at the rotor rotational speed where the frequencies of these two systems coalesce. Therefore, the aeroelastic stability results will be presented in terms of the damping of the blade first chordwise mode in the rotating frame.

Hover - Collective Sweep

The damping variation of the blade first chordwise mode with collective pitch in hover is presented in Fig. 2. The test data are from the transient analysis results using the chordwise bending moment signal at 0.096R. The data scatter is small for the collective pitch range shown, except at 10 deg. collective pitch. The data scatter is attributed to the nonlinear behavior of the elastomeric dampers. At high collective pitch angles, the amount of recirculation in the wind tunnel is large and contributes to excessively high and unsteady blade loadings. High blade loads limited the magnitudes of the excitation level sufficient for stability testing. For bearingless rotors with elastomeric dampers, the level of excitation used in stability testing can strongly affect the transient response behavior of the chordwise modes. Four stability data points were acquired at the 10 deg. collective pitch condition. Damping estimates using the moving block method and the transient analysis for both the chordwise bending moment and the damper displacement are shown in Table 2. Of these four data points, two were acquired at a low excitation level, and the other two at a higher excitation level. The excitation levels shown in Table 2 are given in terms of the initial damper displacement, taken at the time when the excitation level was terminated. The data shown in Table 2 clearly indicate the higher damping estimates are proportional to the higher excitation levels. At small strain levels, the elastomeric damper is stiffer and less effective as a damper than at higher strain levels. The change in damper effectiveness is due both to the damper lower loss factor at small strain levels and also, indirectly, to the increased damper stiffness. A stiffer damper decreases the amount of damper motion per degree of blade lag angle for the first lag mode. Consequently, the damper will contribute less damping to the lag mode for small motions than when operating at the design strain level. Also, as shown in Table 2, the damping estimates from the damper displacement are consistently higher than those obtained from the chordwise bending moment.

Computed damping values using the DART and UMARC analyses are also shown in Fig. 2. The DART results compare well with the measured damping variation, showing a quadratic variation in damping with collective that matches well with the trend of the test data. UMARC results match the test data for most of the range of collective pitch shown. For the collective pitch range below 2 deg., both analyses calculate higher damping levels than the test results. The lower measured damping levels for these points are the result of insufficient chordwise excitation. At low collective pitch settings, because of the small Coriolis coupling, exciting the lag mode with pitch inputs is more difficult than at higher collective pitch settings. The Coriolis coupling is proportional to the blade coning angle, which is small at low collective. The problem was exacerbated for the MDART rotor because control system limits established for the wind tunnel test allowed for little extra dynamic motion when the collective pitch setting was low.

Speed Sweep at Nominal Thrust

Figure 3 shows the damping variation of the MDART rotor with airspeed at $C_T/\sigma = 0.075$. The shaft angle schedule was pre-calculated to simulate steady level flight conditions. The data are from the transient analysis method for the

chordwise bending moment signal. The data scatter is small for the complete range of airspeeds shown. The test data clearly show the MDART rotor has sufficient damping for forward flight operation. The damping level drops gradually from 5 percent critical at hover to a minimum of 3 percent critical at 100 kts and increases moderately at the higher airspeeds. This damping variation is similar to the collective pitch variation with airspeed, except for a small reduction in damping at 100 kts.

Correlation results comparing the UMARC and DART analyses with test data are also presented in Fig. 3. In the UMARC analysis, the Constant Coefficient Approximation method was used to calculate the rotor damping for airspeed below 80 knots ($\mu = 0.20$), while the Floquet-Lyapunov method was used for the higher airspeeds. Both analyses capture the overall trends, with UMARC providing a more conservative calculation. UMARC results overestimate the damping for the airspeed range below 100 kts; at the higher airspeeds, the UMARC results underestimate the test data. DART overestimates the damping values for the complete speed range, with growing deviation at airspeeds beyond 83 kts.

Collective Sweep in Forward Flight

Figure 4 shows the damping variation with collective pitch at 83 kts ($\mu = 0.20$) and at 5.5 deg. forward shaft tilt. Both the moving block and the transient analyses results are shown. For the range of data shown, the damping increases almost linearly with the collective pitch angle. The effect of collective pitch on the chordwise damping at 104 kts ($\mu = 0.25$) is presented in Fig. 5 for a forward shaft tilt of 7.3 deg. The data scatter from both analyses is minimal. The damping increases moderately for the lower collective pitch range and increases sharply for collective pitch angles above 7.4 deg. The increase in damping is attributed to the favorable flap-lag and pitch-lag couplings of the rotor blade at high collective pitch.

Damper Effectiveness with Collective

The strong dependence of the MDART rotor inplane damping with collective pitch is illustrated in Figs. 6 and 7, where all 283 stability data points are presented. Figure 6 shows results using the transient analysis technique and Fig. 7 shows the moving block results. The moving block results have less scatter than do the transient analysis results. Since both methods extract linear approximations from a nonlinear system response, the data scatter shown in Fig. 6 does not imply that the transient analysis is less accurate than the moving block method, but rather this analysis should be considered as being more sensitive to nonlinear system behaviors.

Both Figs. 6 and 7 show that the chordwise damping increases with increasing collective pitch angle. The minimum damping level is about 1 percent critical at the low collective pitch, while the maximum damping level is in excess of 8 percent critical at high collective pitches. The lower damping levels for a given collective pitch generally correspond to the less negative shaft angle tested. A least-squares curve fit of the data reveals a linear variation of damping versus collective for the collective pitch range above 5 deg. The dependence of damping level on rotor thrust was also examined, revealing no particular relationship.

Conclusions

1. The MDART rotor has sufficient inplane damping for all wind tunnel conditions tested.

2. The inplane damping for the MDART rotor depends strongly on the collective pitch angle, with the damping levels increasing with increasing collective pitch angle.

3. The minimum inplane damping level in forward flight at $C_T/\sigma = 0.075$ is approximately 3 percent critical at 100 kts airspeed. The inplane damping increases at the higher airspeeds.

4. In hover, both DART and UMARC results compare well with the measured inplane damping for the MDART rotor. DART results exhibit a trend that compares well with the measured damping; UMARC results match the test data. In forward flight, DART overestimates the measured damping, while the UMARC results are more accurate.

References

1. Bielewa, R. L., Cheney, M. C., Jr., and Novak, R. C., "Investigation of a Bearingless Rotor Concept Having a Composite Primary Structure," NASA CR-2637, Oct 1976.
2. Harris, F. D., Cancio, P. A., and Dixon, P. G., "The Bearingless Main Rotor," Third European Rotorcraft and Powered-Lift Aircraft Forum, Aix-en-Provence, France, Sep 1977.
3. Mychalowycz, E., "Integrated Technology Rotor/Flight Research Rotor Preliminary Design," AVSCOM TR-86-D-8, Mar 1987.
4. Sorensen, J. L., Silverthorn, L. J., and Maier, T. H., "Dynamic Characteristics of Advanced Bearingless Rotors at McDonnell Douglas Helicopter Company," American Helicopter Society 44th Annual Forum, Washington, D. C., Jun 1988.
5. Weller, W. H., "Relative Aeromechanical Stability Characteristics for Hingeless and Bearingless Rotors," *Journal of the American Helicopter Society*, Vol. 35, (3), Jul 1990.
6. Huber, H. and Schick, S., "MBB's BO-108 Design and Development," American Helicopter Society 46th Annual Forum, Washington, D. C., May 1990.
7. Weller, W. H. and Peterson, R. L., "Inplane Stability Characteristics for an Advanced Bearingless Main Rotor

Model," *Journal of the American Helicopter Society*, Vol. 29, (3), Jul 1984.
8. Wang, J. M., Chopra, I., Samak, D. J., Green, M. D., and Graham, T., "Theoretical and Experimental Investigation of the Aeroelastic Stability of an Advanced Bearingless Rotor in Hover and Forward Flight," American Helicopter Society National Specialists' Meeting on Rotorcraft Dynamics, Arlington, TX, Nov 1989.
9. Warmbrodt, W., McCloud, J. L., III, Sheffler, M., and Staley, J., "Full-Scale Wind Tunnel Test of the Aeroelastic Stability of a Bearingless Main Rotor," *Vertica*, Vol. 6, (3), 1982.
10. Ichihashi, T. and Bandoh, S., "Design, Fabrication and Testing of the Composite Bearingless Rotor System for Rotary-Wing Aircraft," Eighteenth European Rotorcraft and Powered-Lift Aircraft Forum, Avignon, France, Sep 1992.
11. McNulty, M., Jacklin, S., and Lau, B., "A Full-Scale Test of the McDonnell Douglas Advanced Bearingless Rotor in the NASA Ames 40 X 80 Foot Wind Tunnel," American Helicopter Society 49th Annual Forum, St. Louis, MO, May 1993.
12. Bousman, W. and Winkler, D., "Application of the Moving Block Analysis," AIAA/ASME/ ASCE/AHS 22nd Structures, Structural Dynamics and Materials Conference, Atlanta, GA, Apr 1981.
13. Wilcox, P. and Crawford, W., "A Least Squares Method for the Reduction of Free Oscillation Data," NASA TN D-4503, Jun 1968.
14. Bir, G. S., Chopra, I., and Nguyen, K., "Development of UMARC (University of Maryland Advanced Rotorcraft Code)," American Helicopter Society 46th Annual Forum, Washington, D. C., May 1990.
15. Johnson, W., "A Comprehensive Analytical Model of Rotorcraft Aerodynamics and Dynamics, Part I: Analysis and Development," NASA TM-81182, Jun 1980.
16. Richards, J. A., *Analysis of Periodically Time-Varying Systems*, Springer-Verlag Berlin, Heidelberg, 1983, pp. 20-22.

Table 1. Computed blade natural frequencies (RPM = 392).

	DART (per rev)	UMARC (per rev)
First Chord	.609	.630
First Flap	1.043	1.054
Second Flap	2.654	2.710
Second Chord	4.377	4.197
Third Flap	4.488	4.630
First Torsion	6.440	6.440

Table 2. Effects of excitation levels on damping estimates. (Hover, 10 deg. collective pitch)

Initial Damper Displacement, in	Damping (% critical) Chordwise Bending Moment		Damping (% critical) Damper Displacement	
	Moving Block	Transient	Moving Block	Transient
.042	4.62	3.79	6.80	5.89
.036	4.21	3.79	4.58	4.79
.074	7.81	8.06	10.70	8.51
.053	9.03	8.68	10.72	10.28

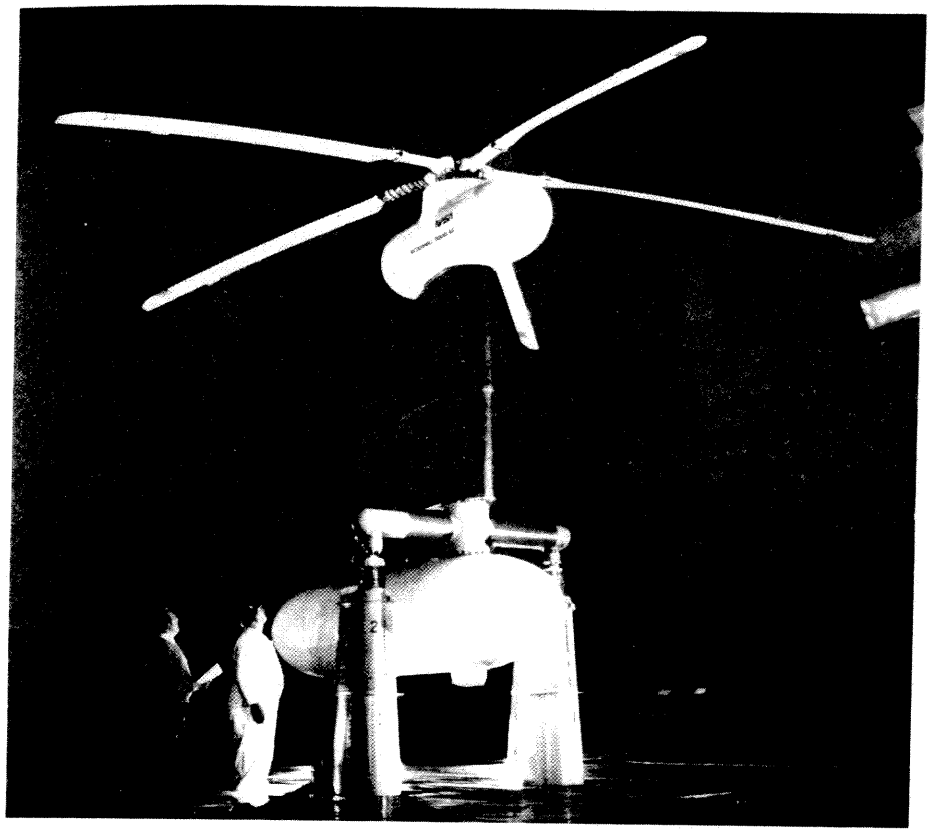

Fig. 1. MDART rotor in the 40- by 80-Foot Wind Tunnel.

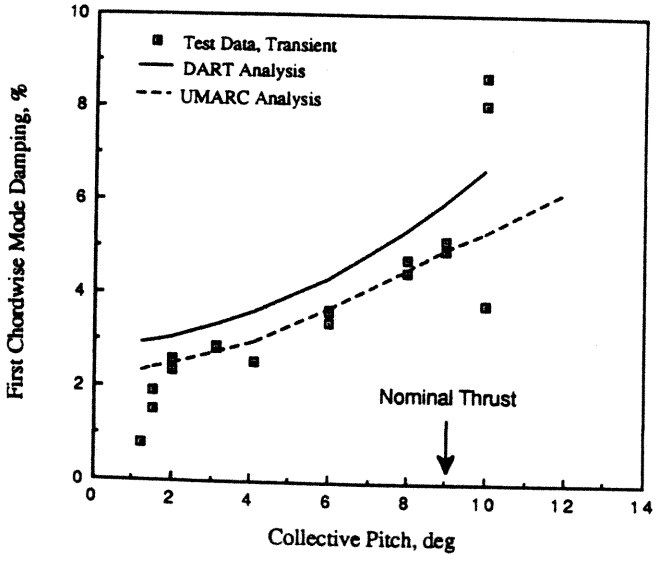

Fig. 2. Blade inplane stability in hover, collective pitch sweep. Analytical results included.

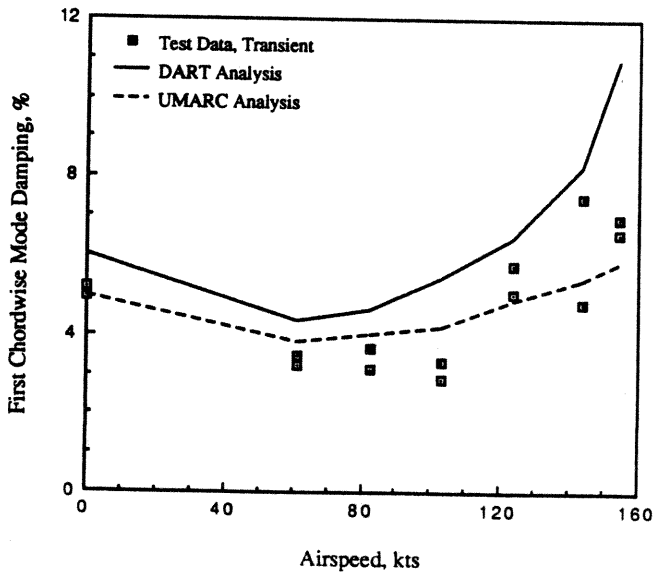

Fig. 3. Variation of blade inplane damping with airspeed at $C_T/\sigma = 0.075$. Analytical results included.

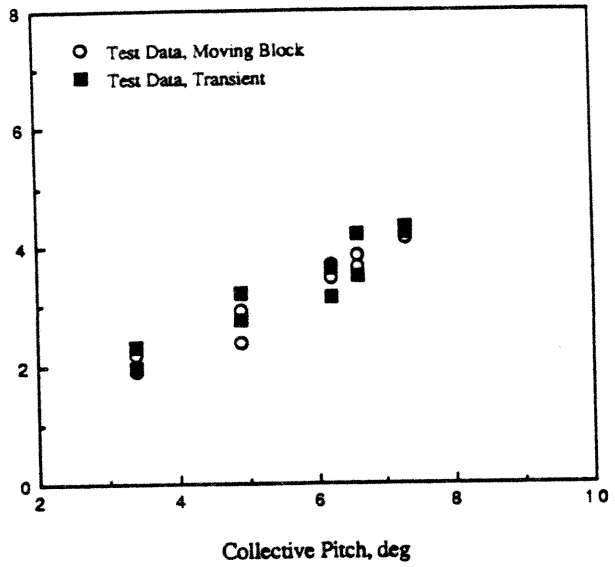

Fig. 4. Variation of rotor inplane stability with collective pitch at 83 kts, 5.5 deg. forward shaft tilt.

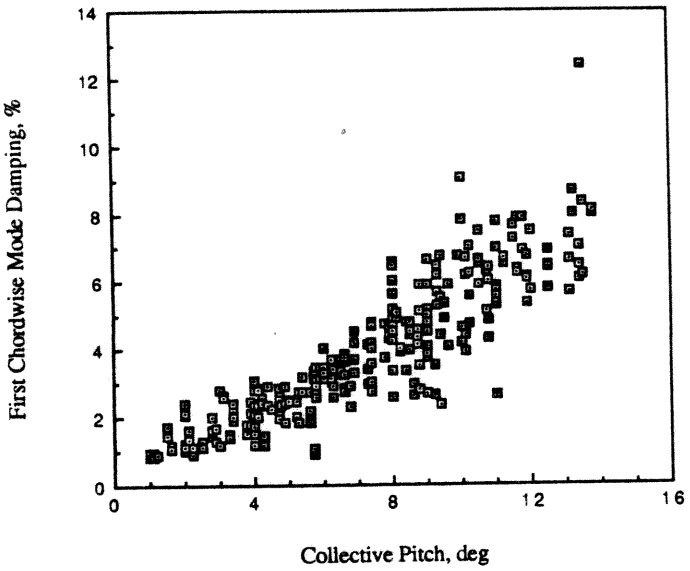

Fig. 6. Variation of rotor inplane damping with collective pitch, all moving block data shown.

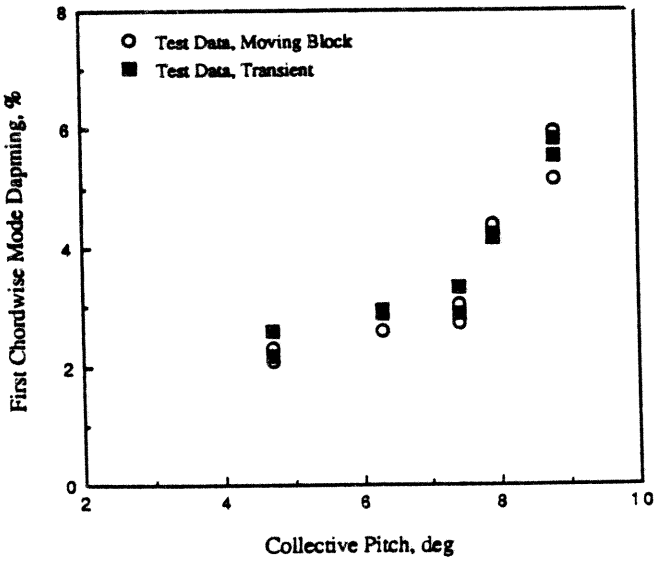

Fig. 5. Variation of rotor inplane damping with collective pitch at 104 kts, 7.3 deg. forward shaft tilt.

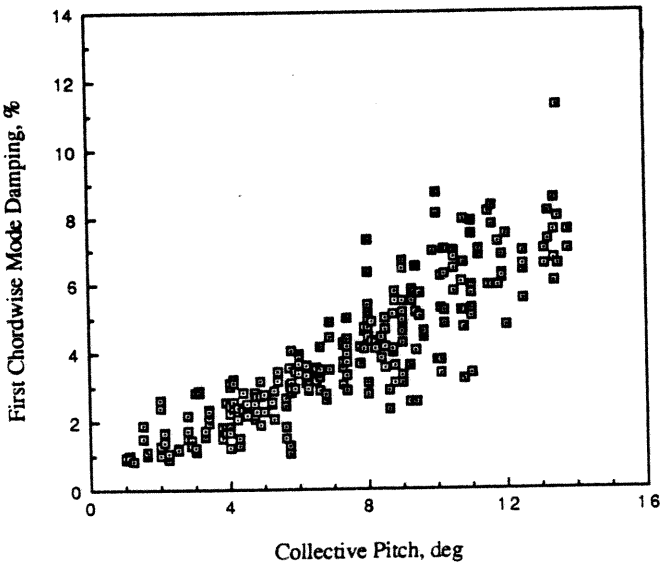

Fig. 7. Variation of rotor inplane damping with collective pitch, all transient analysis data shown.